Engineering Science and Technology, an International Journal 20 (2017) 1122–1128

HOSTED BY

Contents lists available at ScienceDirect

Engineering Science and Technology, an International Journal

journal homepage: www.elsevier.com/locate/jestch

Full Length Article

Chemical reaction and heat transfer on boundary layer Maxwell Ferro-fluid flow under magnetic dipole with Soret and suction effects

A. Majeed [a,*], A. Zeeshan [a], R. Ellahi [a,b]

[a] Department of Mathematics and Statistics, FBAS, IIUI, Islamabad 44000, Pakistan
[b] Department of Mechanical Engineering, University of California, USA

ARTICLE INFO

Article history:
Received 10 September 2016
Revised 6 November 2016
Accepted 8 November 2016
Available online 17 November 2016

Keywords:
Heat and mass transfer
Magnetic dipole
Soret effect
Maxwell parameter
Suction

ABSTRACT

In this article, the influence of chemical reaction and heat transfer analysis of Maxwell saturated Ferro-fluid flow over a stretching sheet under the influence of magnetic dipole with Soret and suction effects are investigated. The sheet is assumed to be permeable in a semi-infinite domain. Firstly, partial differential equations of mass, momentum and concentration for the governing flow problem are modelled and converted into a system of differential equations by utilizing similarity approach. Then the solution of resulting non-linear differential equations is solved by efficient Runge-Kutta technique based on shooting algorithm with the help of MATLAB. Effect of all appropriate parameters like ferromagnetic interaction parameter, chemical reaction parameter, Maxwell parameter, Soret number, suction parameter, Maxwell parameter, Schmidt number, and suction parameter on velocity, temperature and concentration field are confirmed through graphs and table. From the present conclusions, it is examined that by increasing the Maxwell parameter there is a decrease in the fluid velocity and boundary layer thickness. On the other hand, the uprising behaviour is prominent for both temperature and concentration profiles. Also predicted that there is an enhancement in skin friction coefficient and rate of heat transfer by enlarging suction parameter, but opposite trend is noted for Sherwood number. Also noted that the values of Prandtl are taken ranges from 0.72 to 10. The Nusselt number increases from 1.09 to 4.80.

1. Introduction

The combined study of heat and mass transfer with a chemical reaction play dynamic role in flow problem and it gained spectacular attention in last decays because of its wider range of applications occurring in nature and engineering process such that human transpiration, nuclear power plants, cooling of electronic equipment, chemical catalytic reactors and processes, gas turbines and several propulsion devices for aircraft, combustion and furnace design, aerodynamic extrusion of plastic sheets, migration of moisture through the air contained in fibrous insulation, filtration, refrigeration, spreading of chemical pollutants in plants and diffusion of medicine in blood veins, metal spinning and drawing plastic films and many other situation. Gangadhar and Bhaskar Reddy [1] examined heat and mass transfer on MHD boundary layer flow over a moving plate through a porous medium with the effect of chemical reaction and suction. Seddeek and Almushigeh [2] studied the influence of chemical reaction and variable viscosity on MHD convective flow and mass transfer past a stretching surface with thermal radiation. Olanrewaju and Makinde [3] have investigated the effects of thermal diffusion on chemically reacting boundary layer flow of heat and mass transfer past a moving vertical plate in the presence of magnetic field and suction/injection.

Kandasamy et al. [4] examined chemical reaction and thermophoresis effect over a convective porous stretching sheet in the presence heat source/sink. Postelnicu [5] has considered the effect of chemical reaction with Soret and Dufour effects on a porous surface in the absence of magnetic field. Makinde and Olanrewaju [6] studied unsteady mixed convection flow over a porous flat plate moving through a binary mixture embedded with radiative heat transfer and nth-order Arrhenius type of irreversible chemical reaction and considering Dufour and Soret effects. Makinde et al. [7] analyzed the combined influence of buoyancy force, convective heating, Brownian motion, thermophoresis and magnetic field on stagnation-point flow and heat transfer of nanofluid flow along a stretching/shrinking sheet. They establish that both the skin-friction coefficient and the local Sherwood number decrease while the local Nusselt number increases with increasing intensity of buoyancy force.

* Corresponding author.
E-mail address: mjaaqib@gmail.com (A. Majeed).
Peer review under responsibility of Karabuk University.

http://dx.doi.org/10.1016/j.jestch.2016.11.007
2215-0986/

The non-Newtonian fluids fascinated many researchers because of great importance in nature and engineering process, especially in the field of polymer depolarization, bubble columns, electronic chips, fermentation, boiling, composite processing, and application of paints, food processing and many others. The behaviour of Non-Newtonian fluid flow differs from Newtonian fluids. Due to complexity, there is no single constitutive relation available that signifying properties of such types of fluids. The majority of non-Newtonian models available are power law and grade two or three in the literature [8–13]. But the simplest model is the Maxwell model which is suggested by James Clerk Maxwell in 1867. After a few years the knowledge of Maxwell was promoted by James G. Oldroyd (see [14]). Hayat et al. [15] examined heat and mass transfer characteristic of Maxwell fluid through a porous shrinking surface with the existence of the induced magnetic field. Fetecau et al. [16] studied the oscillatory nature of rigid body and unsteady boundary layer flow over a stretching sheet. Also pointed out that Maxwell fluid agrees on relaxation effects which cannot be predictable in other types of non-Newtonian fluids. Adegbie et al. [17] presented the characteristics of upper convected Maxwell Fluid flow over a melting surface with variable thermo-physical properties. Nadeem et al. [18] reported the numerical solutions of non-Newtonian nanofluid flow past a stretching surface using the Maxwell fluid model. Makinde [19] studied the mixed convection flow of an incompressible Boussinesq fluid under the combined action of buoyancy and transverse magnetic field with Soret and Dufour effect over a vertical porous plate with constant heat flux.

All the works mentioned previously are limited to clean fluids, but in the current study, we have considered the Maxwell ferrofluid. In fact, a liquid which is highly magnetized with the magnetic field called ferrofluid. Ferrofluids were first developed and classified in 1963 by Stephen Pappell [20] at the National Aeronautics and Space Administration (NASA). Ferrofluids are a colloidal mixture of liquid and nanoscale ferromagnetic particles suspended uniformly in a single domain non-magnetic carrier fluid [21]. Each tiny particle is systematically coated with a surfactant to prevent agglomeration due to magnetic interactions. These particles have an average size of about 10. It has remarkable applications in recent time due to its significance in micro electro mechanical system (MEMS), purification of molten metals, microfluidic actuators, coolers of nuclear reactors, shock absorbers, leak-proof seals, microfluidic valves and pumps, lithographic patterning and many others [22–26]. Neuringer [27] examined the impact of magnetic field on stagnation point flow of ferrofluid against a cold wall and parallel flow of a heated ferrofluid towards a wall. Sheikholeslami and Gorji [28] recognized ferrofluid flow in a cavity the occurrence of an external magnetic field. Sheikholeslami et al. [29] considered thermal radiation and thermos-mechanical effect of ferrofluid in a semi-annulus enclosure. They also considered the combined influence of ferrohydrodynamic and magnetohydrodynamic. The natural convective flow of ferrofluid the in a cavity is performed by Kefayati [30]. He noticed that heat transfer rate decreases by an increasing volume fraction of ferromagnetic particles. Feng et al. [31] presented an experimental study for controlling the acoustically heat transfer of a ferromagnetic fluid. Rashidi et al. [32] performed mixed convection flow and heat transfer analysis of nanofluid in a channel. A number of studied related to ferromagnetic fluid were executed by the researcher [33–36].

The above literature survey inspires the present study, which aims to discuss the influence of magnetic dipole and heat generation and absorption on boundary layer Maxwell saturated ferrofluid. The transformed coupled differential equations are solved by Runge-Kutta algorithm. The impact of numerous pertinent parameters is deliberated thoroughly pictorially.

2. Mathematical formulation

2.1. Magnetic dipole

Magnetic liquid flow is influenced by the dipole field whose permanent magnetic scalar potential is taken as

$$\Phi = \frac{\gamma}{2\pi}\left(\frac{x}{x^2+(y+a)^2}\right) \tag{1}$$

where γ is the strength of magnetic field. The components of magnetic field intensity H_x and H_y along the coordinates x and y axes are

$$H_x = -\frac{\partial\Phi}{\partial x} = \frac{\gamma}{2\pi}\left\{\left(\frac{x^2-(y+a)^2}{(x^2+(y+a)^2)^2}\right)\right\} \tag{2}$$

$$H_y = -\frac{\partial\Phi}{\partial y} = \frac{\gamma}{2\pi}\left\{\left(\frac{2x(y+a)}{(x^2+(y+a)^2)^2}\right)\right\} \tag{3}$$

Magnetic field intensity H is stated as

$$H = \left[\left(\frac{\partial\Phi}{\partial x}\right)^2 + \left(\frac{\partial\Phi}{\partial y}\right)^2\right]^{\frac{1}{2}} \tag{4}$$

$$\frac{\partial H}{\partial x} = -\frac{\gamma}{2\pi}\left(\frac{2x}{(y+a)^4}\right) \tag{5}$$

$$\frac{\partial H}{\partial y} = \frac{\gamma}{2\pi}\left(\frac{-2}{(y+a)^3} + \frac{4x^2}{(y+a)^5}\right) \tag{6}$$

Magnetization M can be considered as a linear function of temperature T [37].

$$M = K^*(T_c - T) \tag{7}$$

where K^* is pyromagnetic coefficient and T_c is Curie temperature, however, the following point is essential for the occurrence of ferrohydrodynamic interaction: (i) the fluid is at a temperature T different from T_c and (ii) the external magnetic field is inhomogeneous. Once the ferromagnetic fluid approaches Curie temperature, there is no furthermore magnetization. Characteristic for physical significance is very important is very important, as Curie temperature is very large, that is 1043 Kelvin for iron.

2.2. Flow analysis

Let us consider two-dimensional, Maxwell ferrofluid electrically non-conducting along with heat and mass transfer past a stretching surface under the impact of external magnetic field induced by the dipole. A permeable stretching sheet is considered along with the x-axis with velocity u_w and y-axis is measured normal to the sheet as seen schematically in Fig. 1. A magnetic dipole is situated in the center of y-axis and distance "a" from the sheet. Owing to a dipole, magnetic field point in the positive x-direction and rising the magnetic field strength to marinate the ferrofluid. It is also supposed that uniform temperature at the surface is T_w and Curie temperature T_c, while ambient temperature $T_\infty = T_c$ and concentration C_∞ far away from the surface sheet.

By introducing Boussineq's boundary layer approximations, the governing equations for Maxwell saturated ferro-fluids are:

$$\frac{\partial u}{\partial x} + \frac{\partial v}{\partial y} = 0, \tag{8}$$

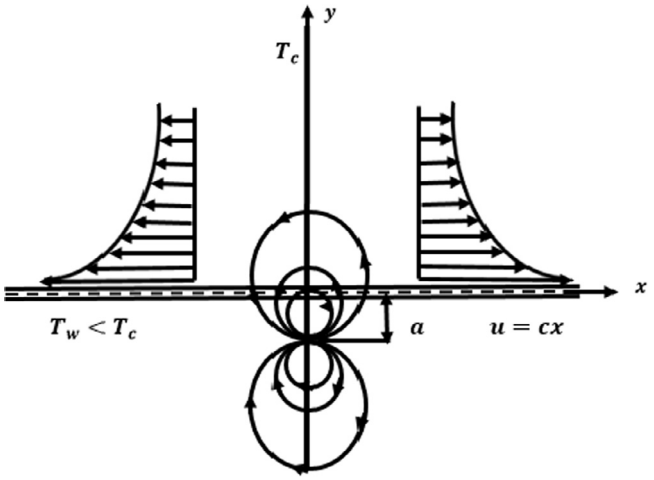

Fig. 1. The geometry of the problem, circles indicate magnetic dipole.

$$u\frac{\partial u}{\partial x}+v\frac{\partial u}{\partial y}+\lambda_1\left(u^2\frac{\partial^2 u}{\partial x^2}+v^2\frac{\partial^2 u}{\partial y^2}+2uv\frac{\partial^2 u}{\partial x\partial y}\right)=\frac{\mu_0}{\rho}M\frac{\partial H}{\partial x}+v\frac{\partial^2 u}{\partial y^2}, \tag{9}$$

$$\left(u\frac{\partial T}{\partial x}+v\frac{\partial T}{\partial y}\right)+\frac{\mu_0 T}{\rho c_p}\frac{\partial M}{\partial T}\left(u\frac{\partial H}{\partial x}+v\frac{\partial H}{\partial y}\right)=\frac{k}{\rho c_p}\frac{\partial^2 T}{\partial y^2}+\frac{k}{\rho c_p}\left[\mu\left(\frac{\partial u}{\partial y}\right)^2+2\mu\left(\frac{\partial v}{\partial y}\right)^2\right]+\frac{Dk_T}{c_s c_p}\frac{\partial^2 C}{\partial y^2} \tag{10}$$

$$\left(u\frac{\partial C}{\partial x}+v\frac{\partial C}{\partial y}\right)=D\frac{\partial^2 C}{\partial y^2}-k_0(C-C_\infty)+\frac{Dk_T}{T_m}\frac{\partial^2 T}{\partial y^2} \tag{11}$$

where (u, v) are velocity component of fluid along coordinate axes, λ_1 is relaxation time, C and T is concentration and temperature of fluid, ρ is density of the fluid, c_S is concentration susceptibility, μ is dynamic viscosity, v is kinematic viscosity, μ_0 is magnetic permeability, k and c_P are thermal conductivity and specific heat of fluid, D is mass diffusivity, k_T is thermal diffusion ration, k_0 is chemical reaction rate on the species concentration, M is magnetization, H is magnetic field strength, T_m is mean fluid temperature.with appropriated boundary conditions are

$$u=u_w=cx,\quad v=v_w,\quad T=T_w=T_c-A\left(\frac{x}{l}\right)^2 C=C_w aty=0 \tag{12}$$

$$u\to 0,\quad \frac{\partial u}{\partial y}\to 0,\quad T\to T_c,\quad C\to C_\infty \text{ as } y\to\infty \tag{13}$$

where $c>0$ is the stretching rate of the sheet, v_w is the suction/injection velocity. A is positive constant and $l=\sqrt{v/c}$ is the characteristic length.

3. Solution procedure

Introducing the similarity transformation assumed by [37]

$$\Psi=\left(\frac{\mu}{\rho}\right)\xi.f(\eta),\quad \theta=\frac{T_c-T}{T_c-T_w}=\theta_1(\eta)+\xi^2\theta_2(\eta),\quad \phi=\frac{C-C_\infty}{C-C_w} \tag{14}$$

where

$$T_c-T_w=A\left(\frac{x}{l}\right)^2,\quad \xi=\sqrt{\frac{c\mu}{\rho}}x \text{ and } \eta=\sqrt{\frac{c\mu}{\rho}}y \tag{15}$$

$\Psi(\xi,\eta)$ *and* $\theta(\xi,\eta)$ are stream function and temperature. The components of velocity are taken as

$$u=\frac{\partial\Psi}{\partial y}=cx.f'(\eta),\quad v=-\frac{\partial\Psi}{\partial x}=-\sqrt{cv}.f(\eta) \tag{16}$$

Substituting Eqs. (14)–(16) into the Eqs. (9)–(11), and comparing coefficients of like powers of ξ, up to ξ^2, we get:

$$f'''(1-\gamma_1 f^2)-(f'^2-ff')+2\gamma_1 ff'f'-\frac{2\beta\theta_1}{(\eta+\alpha_1)^4}=0, \tag{17}$$

$$\theta_1''+\Pr(f\theta_1'-2f'\theta_1)+\frac{2\lambda\beta(\theta_1-\varepsilon)f}{(\eta+\alpha_1)^3}-2\lambda f'^2-D_r\phi'=0, \tag{18}$$

$$\theta_2''-\Pr(4f'\theta_2-f\theta_2')+\frac{2\lambda\beta\theta_2 f}{(\eta+\alpha_1)^3}-\lambda\beta(\theta_1-\varepsilon)\left[\frac{2f'}{(\eta+\alpha_1)^4}+\frac{4f}{(\eta+\alpha_1)^5}\right]-\lambda f'^2=0, \tag{19}$$

$$\phi'+S_c(f\phi'-k_1\phi+S_r\theta_1')=0, \tag{20}$$

The initial and boundary conditions (12) and (13) are renovated as

$$f=S,\quad f'=1,\quad \theta_1=1,\quad \theta_2=0,\quad \phi=1,\ \text{at } \eta=0 \tag{21}$$

$$f'\to 0,\quad \theta_1\to 0,\quad \theta_2\to 0,\quad \phi\to 0 \text{ as } \eta\to\infty \tag{22}$$

The non-dimension quantities occur in Eqs. (17)–(20) are

$$\left.\begin{aligned}&\beta=\tfrac{\gamma\rho}{2\pi\mu^2}\mu_0K^*(T_c-T_w),\quad \gamma_1=\lambda_1 c,\quad \lambda=\tfrac{c\mu^2}{\rho k(T_c-T_w)},\\ &\Pr=\tfrac{\mu c_p}{k},\quad S=\tfrac{-v_w}{\sqrt{cv}},\quad \alpha_1=\sqrt{\tfrac{c\rho}{\mu}}a,\quad \varepsilon=\tfrac{T_c}{T_c-T_w},\\ &S_r=\tfrac{Dk_T(C_\infty-C_w)}{T_m v(T_c-T_w)},\quad K_1=\tfrac{k_0}{c},\quad S_c=\tfrac{v}{D},\end{aligned}\right\} \tag{23}$$

where β is ferromagnetic interaction parameter, γ_1 is Maxwell parameter, λ is viscous dissipation parameter, S_c is Schmidt number, Pr is Prandtl number, S is a suction parameter, α_1 is the dimensionless distance from the origin to the dipole and ε is the dimensionless Curie temperature ratio, S_r in the Soret number, K_1 is the chemical reaction parameter.

Concerning physical quantities of practical interest are skin-friction coefficient, heat transfer rate and Sherwood number, which can be expressed as:

$$C_{f_x}=\frac{-\tau_w}{\rho(cx)^2},\quad Nu_x=\frac{xq_w}{-k(T_c-T_w)},\quad Sh_x=\frac{xJ_w}{D_e(C_w-C_\infty)} \tag{24}$$

where τ_w is shear stress, q_w is heat flux and J_w is mass flux

$$\tau_w=\mu(1+\gamma_1)\left(\frac{\partial u}{\partial y}\right)_{y=0},\ q_w=-\left(\frac{\partial T}{\partial y}\right)_{y=0},\ J_w=-D_e\left(\frac{\partial C}{\partial y}\right)_{y=0} \tag{25}$$

Using the relation Eqs. (14)–(16) we can obtain

$$\left.\begin{aligned}&C_f\mathrm{Re}_x^{1/2}=-(1+\gamma_1)f'(0),\\ &Nu_x/\mathrm{Re}_x^{1/2}=-(\theta_1'(0)+\xi^2\theta_2'(0)),\\ &Sh_x/\mathrm{Re}_x^{1/2}=-\phi'(0)\end{aligned}\right. \tag{26}$$

4. Numerical solution

Eqs. (17)–(20) along with transformed boundary conditions (21) and (22) are nonlinear two-point boundary value problem (BVP) which are difficult to solve analytically, must be solved numerically by applying fourth order efficient Runge-Kutta method based shooting algorithm with the help of MATLAB software for some values of leading parameters β, S, γ_1, K_1, S_c, and S_r.

The reduced system of first-order ODE's, are then solved as an initial value problem (IVP). For this assume that $y_1 = f, y_2 = f', y_3 = f'', y_4 = \theta_1, y_5 = \theta_1', y_6 = \theta_2, y_7 = \theta_2', y_8 = \phi, y_8 = \phi'$. The transformed equations are as follows.

$$
\begin{aligned}
y_1' &= y_2,\\
y_2' &= y_3,\\
y_3' &= \frac{1}{(1-\gamma_1 y_1^2)}\left[(y_2^2 - y_1 y_3) - 2\gamma_1 y_2 y_3 + \frac{2\beta y_4}{(\eta+\alpha_1)^4}\right],\\
y_4' &= y_5,\\
y_5' &= -\mathrm{Pr}(y_1 y_5 - 2y_2 y_4 - Q y_4) - \frac{2\lambda\beta y_1 (y_4 - \varepsilon)}{(\eta+\alpha_1)^3} + 2\lambda y_2^2,\\
y_6' &= y_7,\\
y_7' &= \mathrm{Pr}(4y_2 y_6 - y_1 y_7 - Q y_6) - \frac{2\lambda\beta y_1 y_6}{(\eta+\alpha_1)^3}\\
&\quad - \lambda\beta(y_4 - \varepsilon)\left[\frac{2y_2}{(\eta+\alpha_1)^4} + \frac{4y_1}{(\eta+\alpha_1)^5}\right] + \lambda y_3^2,\\
y_8' &= y_9,\\
y_9' &= -S_c(y_1 y_9 - K_1 y_8 + S_r y_5'),
\end{aligned}
\tag{27}
$$

and the corresponding initial conditions are

$$y_1(0) = 0, \quad y_2(0) = 1, \quad y_3(0) = s_3,$$

$$y_4(0) = 1, \quad y_5(0) = s_5, \quad y_6(0) = 0,$$

$$y_7(0) = s_7, \quad y_8(0) = 1, \quad y_9(0) = s_9,$$

where $s_3, s_5\ s_7$ and s_9 are unknown conditions value for $f''(0), \theta_1'(0)$, $\theta_2'(0)$ and $\phi'(0)$ which are not given, but we have an additional endpoint conditions $y_2(\infty) = 0, y_4(\infty) = 0, y_6(\infty) = 0, y_8(\infty) = 0$. Choose suitable initial guess for $f''(0), \theta_1'(0), \theta_2'(0)$ and $\phi'(0)$ in such a way that system of first order ODE's fulfil the endpoint conditions and found the desired solution for Eq. (27). Select $\eta_{\max} = 15$ with simulation error is chosen 10^{-5} in order to assure asymptotic convergence.

5. Results and discussion

In this part, comprehensive numerical computations are conducted for several pertinent governing constraints that designate the flow pattern and results are demonstrated through pictorially and tabular form. Figures are drawn for velocity, temperature, and concentration profiles against ferromagnetic interaction parameter, Soret number, chemical reaction parameter, Maxwell parameter, Schmidt number, and suction parameter. The values of the emerging parameter throughout the problem are taken as $\mathrm{Pr} = 2$, $\beta = 0.1$, $\gamma_1 = 0.1$, $\lambda = 0.01$, $S = 0.1$, $S_r = 0.5$, $S_c = 0.5$, $K_1 = 0.2$, $\varepsilon = 2.0$, $\alpha_1 = 1.0$. The comparison is given in Table 1, showing a marvellous agreement with the published data.

Fig 2. Illustrate the concentration profile for some values of the Soret number. From the figure it is perceived that increase in the value of *Sr*, concentration of fluid is growing boundary layer region due to the involvement of temperature gradients in species diffusion increases the concentration.

Table 1
Comparison of Nusselt number for the case of $\beta = \lambda = \gamma_1 = S = K_1 = S_r = S_c$.

Pr	Abel et al. [12]	Zeeshan et al. [36]	Chen [38]	Present results
0.72	1.0885	1.08862	1.0885	1.088527
1	1.3333	1.33333	1.3333	1.333333
3	–	2.50972	2.5097	2.509725
10	4.7968	4.79682	4.7968	4.796873

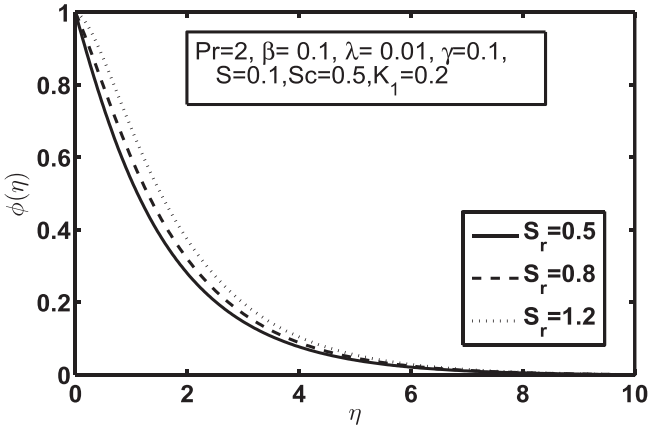

Fig. 2. Influence of Soret number S_r on concentration profile ϕ.

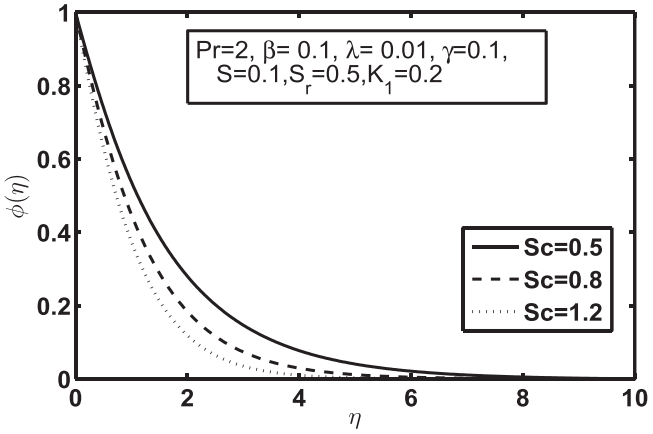

Fig. 3. Influence of Schmidt parameter *Sc* on concentration profile ϕ.

The impact of Schmidt number *Sc* on dimensionless concentration profiles is pointed out in Fig 3. It is simply apparent from the figure that concentration in boundary layer thickness suppressed by enlarging the Schmidt number. By definition, *Sc* is inversely varied to the diffusion coefficient ??. Also observed that *Sc* defined effectiveness of the momentum diffusion in hydrodynamic flow to the species diffusion in concentration field. So higher values of *Sc* causes reduction in concentration field. Chemical reaction parameter shows similar behaviour as the Schmidt number on

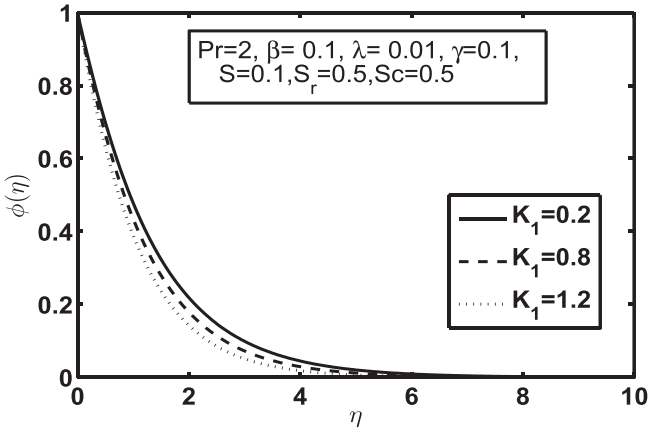

Fig. 4. Influence of chemical reaction parameter K_1 on concentration profile ϕ.

concentration profile. By analyzing the influence of a destructive chemical reaction parameter ($K_1 > 0$) caused a reduction in the concentration diffusion species. Physical point of view chemical reaction for destructive case is very large. Because of this fact molecular motion is quite higher which enhances the transport phenomenon, thus supressing the concentration field in the fluid flow as display in Fig 4.

Figs 5(a)–(c) classify the impact of ferromagnetic interaction parameter on dimensionless velocity, temperature and concentration fields. The outcome of the applied magnetic field due to magnetic dipole demonstrates through a ferromagnetic interaction parameter β. The existence of magnetic effects acts as delaying force on fluid velocity and thereby as increases, so does delaying force and hereafter the results in suppressing the velocity profile $f'(\eta)$ as seen in Fig 5a. In fact, this happens due to the influence of Lorentz force which opposes the flow and produces more resistance to the transport phenomena. Because there is an intervention between the fluid motion and the action of the applied magnetic field. This kind of intervention reduces the velocity and rising the frictional heating involving within the fluid layers which are accountable for the increment in the concentration and heat profiles as cleared in Fig 5b and c.

Figs 6(a)–(c) inaugurate the influence of Maxwell parameter γ_1 on dimensionless velocity, temperature and concentration fields. From figures, it is perceived that when Maxwell parameter increases, then the velocity of the fluid is declined at any point above the sheet and boundary layer thickness decreases for a large

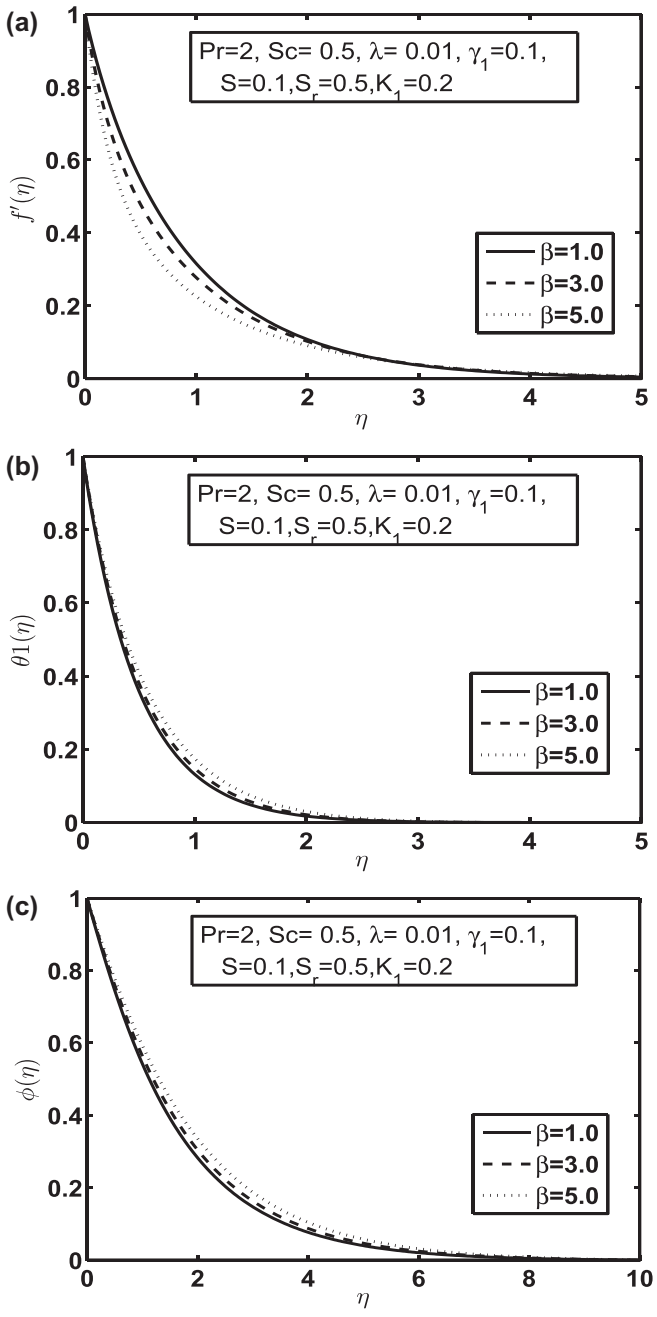

Fig. 5. a. Influence of ferromagnetic interaction parameter β on velocity profile f'. b. Influence of ferromagnetic interaction parameter β on temperature profile θ_1. c. Influence of ferromagnetic interaction parameter β on temperature profile θ_1.

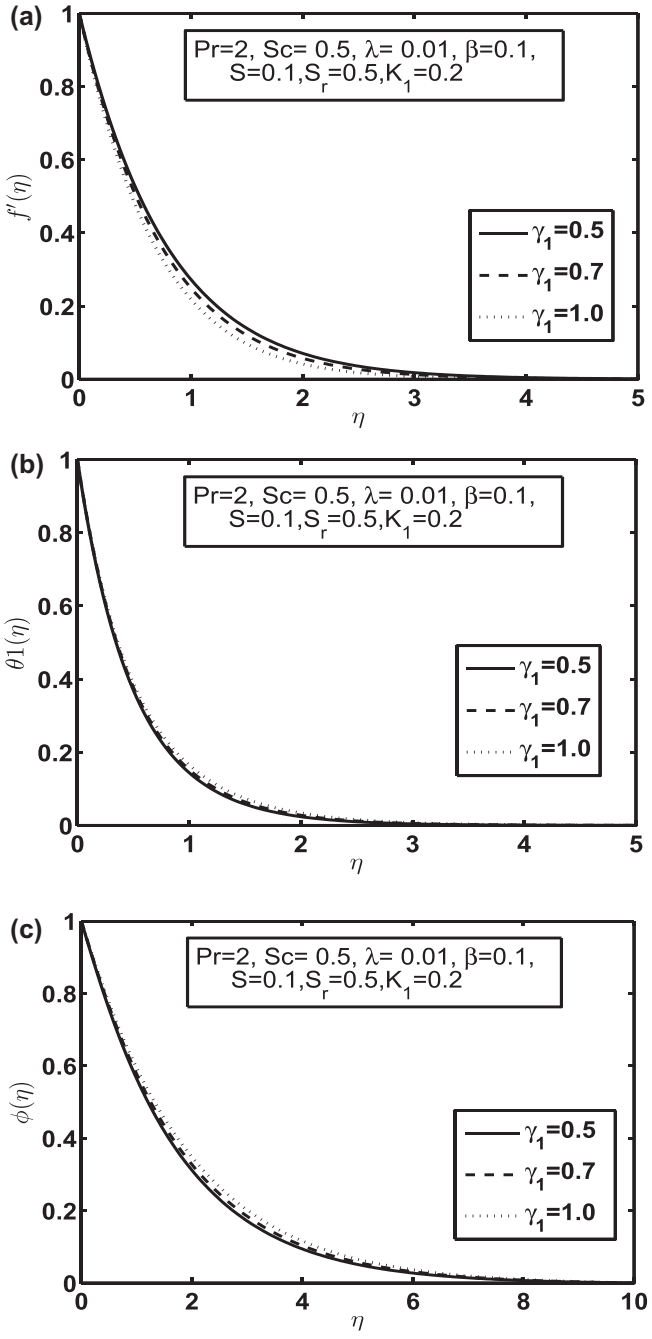

Fig. 6. a. Influence of Maxwell parameter γ_1 on velocity profile f'. b. Influence of Maxwell parameter γ_1 on temperature profileθ_1. c. Influence of Maxwell parameter γ_1 on concentration profile ϕ.

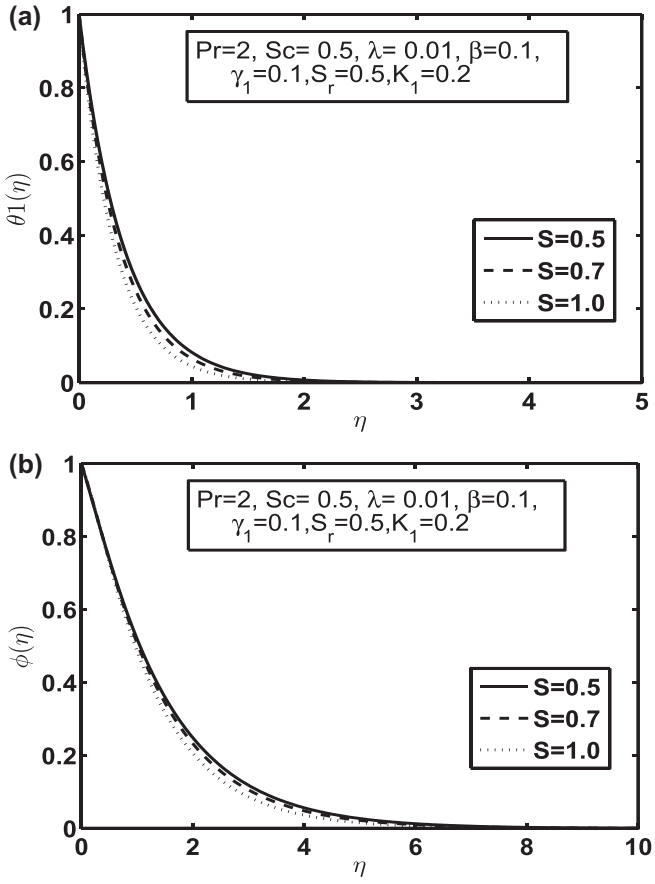

Fig. 7. a. Influence of suction parameter S on temperature profile θ_1. b. Influence of suction parameter S on concentration profile ϕ.

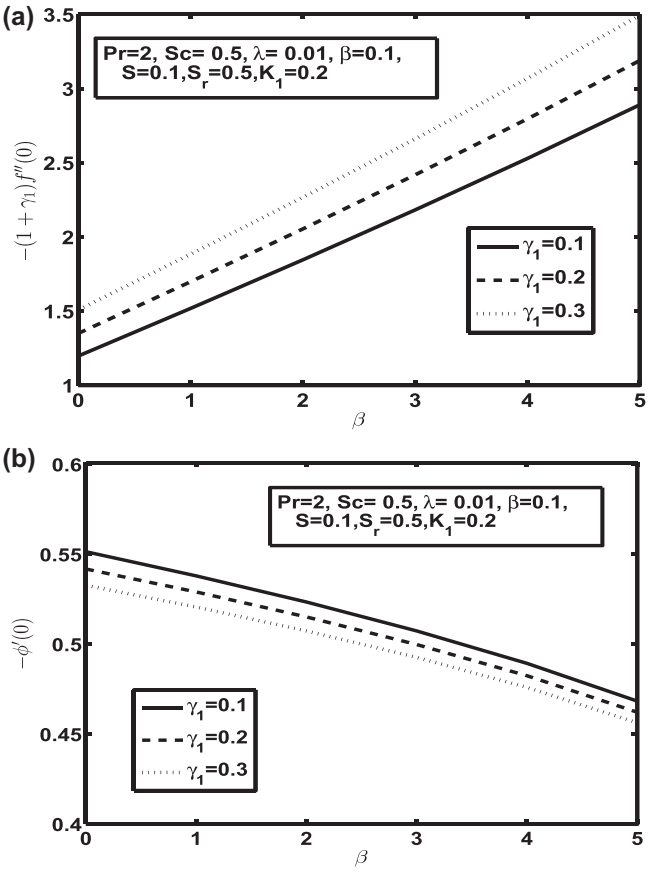

Fig. 8. a. Influence of Maxwell parameter γ_1 on Skin friction coefficient versus β. b. Influence of Maxwell parameter γ_1 on Sherwood number versus β.

value of γ_1. From a physical point of view, when shear stress is eliminated, fluid will come to rest. This sort of phenomena is shown in many polymeric liquids that cannot be defined in the Newtonian fluid model. A large value of Maxwell parameter will produce a retarding force between two adjacent layers in the flow. Due to this, there is a reduction in the velocity and boundary layer thickness as seen in Fig 6a. Also observed that temperature and concentration profile enhances by enlarging the Maxwell parameter because the thickening of the thermal and solute boundary layer happens for increasing the elasticity stress parameter as confirmed in Fig 6b and c.

The influence of suction parameter S on temperature and concentration profile is explained through Fig 7(a)-(b). It is detected that both velocity and concentration decreases expressively by rising suction parameter. This behaviour occurs in the presence of suction at the surface, which is the result to draw the quantity of fluid on the surface and therefore hydrodynamic boundary layer flow becomes thinner and both thermal, and species boundary layer gets slowed down by enlarging suction parameter.

Table 2
Skin friction $-f''(0)$, local Nusselt number $-\theta_1'$ and local Sherwood number $-\varnothing'(0)$ for β, γ_1, S_r, Sc, K_1, S.

β	γ_1	S_r	Sc	K_1	S	$-(1+\gamma_1)f''(0)$	$-\theta_1'(0)$	$-\varnothing'(0)$
0.5	0.1	0.5	0.5	0.2	0.1	0.1336	2.0799	0.5449
0.7						0.1920	2.0733	0.5422
1.2						0.3391	2.0564	0.5352
0.5	0.1	0.5	1.0	0.2	0.1		–	0.7482
			1.5				–	0.8821
			2.0				–	0.9830
0.5	0.5	0.5	0.5	0.2	0.1	0.1301	2.0345	0.5108
	0.7					0.2663	2.0131	0.4962
	1.2					0.6154	1.9620	0.4650
0.5	0.1	0.5	0.5	0.2	0.1		–	0.5449
				0.4			–	0.6250
				0.6			–	0.6950
0.5	0.1	0.5	0.5	0.2	0.2	0.1997	2.1852	0.5324
					0.4	0.3474	2.4095	0.5047
					0.6	0.5189	2.6514	0.4737
0.5	0.1	0.5	0.5	0.2	0.1		–	0.5449
		0.7					–	0.3880
		1.2					–	−0.0044

Fig 8(a)-(b) shows the impact of Maxwell parameter on the skin friction and Sherwood number with the variation of ferromagnetic interaction parameter. The graphs clarify that increasing the values of Maxwell parameter causes increments in the skin friction and decrements in Sherwood number. The physical point of view, at higher Maxwell parameter, the material behaviour changes to a non-Newtonian regime, increasingly dominated by elasticity, demonstrating solid-like behaviour, hence high skin friction.

6. Concluding remarks

In this investigation, the problem of heat and mass transfer with chemical reaction on boundary layer Maxwell Ferro-fluid flow over a stretching surface under the influence of magnetic dipole has been studied. Mathematical equations are modelled and converted into ODE's, then solved numerically by adopting Runge-Kutta based shooting technique with MATLAB package. Some effective governing parameter on the flow problem like chemical reaction parameter (K_1), Maxwell parameter (γ_1) ferromagnetic interaction parameter (β) suction parameter (S), Soret number (S_r) and Schmidt number (S_c) on velocity profile, temperature profile, concentration filed, skin friction coefficient, heat transfer rate and Sherwood number are sketched graphically and elucidated in detail. Heat transfer rate is taken against Pr which is increased approximately 18%, 56.6% and 77% at Prandtl number 1.0, 3.0 and 10. Some of the major observations of the current flow problem are elaborated as follows:

- Fluid velocity is flattening by increasing the values of suction and ferromagnetic interaction parameter.
- Nusselt number and Sherwood number decreases by increasing chemical reaction and ferromagnetic interaction parameter, whereas reverse effect in noted for Skin friction coefficient as seen in Table 2.
- Both concentration and temperature field enhances with increasing Maxwell parameter.
- Rising the values of Schmidt number is to reduce the concentration profile and reverse nature is found for Sort number.

References

[1] K. Gangadhar, N. Bhaskar Reddy, Chemically reacting MHD boundary layer flow of heat and mass transfer over a moving vertical plate in a porous medium with suction, J. Appl. Mech. 6 (2013) 1.
[2] M.A. Seddeek, A.A. Almushigeh, Effects of radiation and variable viscosity on MHD free convective flow and mass transfer over a stretching sheet with chemical reaction, Appl. Math. Comput. 5 (2010) 1.
[3] P.O. Olanrewaju, O.D. Makinde, Effects of thermal diffusion and diffusion thermo on chemically reacting MHD boundary layer flow of heat and mass transfer past a moving vertical plate with suction/injection, Arabian J. Sci. Eng. 36 (2011) 1607–1619.
[4] R. Kandasamy, T. Hayat, S. Obaidat, Group theory trans-formation for Soret and Dufour effects on free convective heat and mass transfer with thermophoresis and chemical reaction over a porous stretching surface in the presence of heat source/sink, Nucl. Eng. Des. 241 (2011) 6.
[5] A. Postelnicu, Influence of chemical reaction on heat and mass transfer by natural convection from vertical surfaces in porous media considering Soret and Dufour effects, Heat Mass Transfer 43 (2007) 6.
[6] O.D. Makinde, P.O. Olanrewaju, Unsteady mixed convection with Soret and Dufour effects past a porous plate moving through a binary mixture of chemically reacting fluid, Chem. Eng. Commun. 198 (7) (2011) 920–938.
[7] O.D. Makinde, W.A. Khan, Z.H. Khan, Buoyancy effects on MHD stagnation point flow and heat transfer of a nanofluid past a convectively heated stretching/shrinking sheet, Int. J. Heat Mass Transfer 62 (2013) 526–533.
[8] M.H. Haroun, Effect of Deborah number and phase difference on peristaltic transport of a third-order fluid in an asymmetric channel, Commun. Nonlinear Sci. Numer. Simul. Commun. Nonlinear Sci. Numer. Simul. 12 (8) (2007).
[9] W.A. Khan, J.R. Culham, O.D. Makinde, Combined heat and mass transfer of third-grade nanofluids over a convectively-heated stretching permeable surface, Can. J. Chem. Eng. 93 (10) (2015) 1880–1888.
[10] B. Serdar, M. Salih Dokuz, Three-dimensional stagnation point flow of a second grade fluid towards a moving plate, Int. J. Eng. Sci. 44 (1) (2006).
[11] A.M. Siddiqui, A. Zeb, Q.K. Ghori, A.M. Benharbit, Homotopy perturbation method for heat transfer flow of a third grade fluid between parallel plates, Chaos Solitons Fractals, Chaos Solitons Fractals 36 (2008) 1.
[12] M.S. Abel, E. Sanjayan, M.M. Nandeppanavar, Viscoelastic MHD flow and heat transfer over a stretchingsheet with viscous and ohmic dissipations, Commun. Nonlinear Sci. Commun. Nonlinear. Sci. Numer. Simul. 13 (9) (2008).
[13] A. Zeeshan, A. Majeed, Heat transfer analysis of Jeffery fluid flow over a stretching sheet with suction/injection and magnetic dipole effect, Alexandria Eng. J. 55 (3) (2016) 2171–2181.
[14] W.M. Christopher, Rheology: Principles, Measurements and Applications, Wiley-VCH Publisher, Weinheim, 1993.
[15] T. Hayat, C. Fetecau, Z. Abbas, N. Ali, Flow of a viscoelastic fluid with fractional Maxwell model between two side walls due to suddenly moved plate, Nonlinear Anal. Real World Appl. 9 (2008) 5.
[16] C. Fetecau, M. Jamil, I. Siddique, A note on the second problem of Stokes for Maxwell fluids, Int. J. Non-Linear Mech. 44 (2009) 10.
[17] K.S. Adegbie, A.J. Omowaye, A.B. Disu, I.L. Animasaun, Heat and mass transfer of upper convected Maxwell fluid flow with variable thermo-physical properties over a horizontal melting surface, Appl. Math. 6 (2015) 8.
[18] S. Nadeem, R. Mehmood, N.S. Akbar, Non-orthogonal stagnation point flow of a nano non-Newtonian fluid towards a stretching surface with heat transfer, Int. J. Heat Mass Transfer 57 (2013) 2.
[19] O.D. Makinde, On MHD Mixed convection with Soret and Dufour effects past a vertical plater embedded in a porous medium, Latin Am. Appl. Res. 41 (1) (2011) 63.
[20] S.S. Papell, Low viscosity magnetic fluid obtained by the colloidal suspension of magnetic particles, United States Patent Office Filed Ser 315 (1965).
[21] R.E. Rosensweig, Ferrohydrodynamics, Dover Publications Inc, New York, 1997.
[22] F. Selimefendigil, H.F. Oztop, Numerical study and pod-based prediction of natural convection in ferrofluids filled triangular cavity with generalized neural networks (grnn), Numer. Int. J. Heat Mass Transfer 78 (2014).
[23] P. Bissell, P. Bates, R. Chantrell, K. Raj, J. Wyman, Cavity magnetic field measurements in ferrofluids, J. Magn. Magn. Mater. 39 (1983) 1–2.
[24] A. Majeed, A. Zeeshan, R. Ellahi, Unsteady ferromagnetic liquid flow and heat transfer analysis over a stretching sheet with the effect of dipole and prescribed heat flux, J. Mol. Liq. 223 (2016) 528–533.
[25] C. Vales-Pinzon, J. Alvarado-Gil, R. Medina-Esquivel, P. Martinez-Torres, Polarized light transmission in ferrofluids loaded with carbon nanotubes in the presence of a uniform magnetic field, J. Magn. Magn. Mater. 369 (2014).
[26] B.B. Yellen, G. Fridman, G. Friedman, Ferrofluid lithography, Nanotechnology 15 (2004) 10.
[27] J.L. Neuringer, Some viscous flows of a saturated ferrofluid under the combined influence of thermal and magnetic field gradients, Int. J. Nonlinear Mech. 1 (1966) 2.
[28] M. Sheikholeslami, M. Gorji-Bandpy, Free convection of ferrofluid in a cavity heated from below in the presence of an external magnetic field, Powder Technol. 256 (2014).
[29] M. Sheikholeslami, D.D. Ganji, M.M. Rashidi, Ferrofluid flow and heat transfer in a semi annulus enclosure in the presence of magnetic source considering thermal radiation, J. Taiwan Inst. Chem. Eng. 47 (2015).
[30] G. Kefayati, Natural convection of ferrofluid in a linearly heated cavity utilizing LBM, J. Mol. Liq. 191 (2014).
[31] Wu Feng, Wu Chih, Guo Fangzhong, Li Duanyong, Acoustically controlled heat transfer of ferromagnetic fluid, Int. J. Heat Mass Transfer 44 (23) (2001).
[32] M.M. Rashidi, M. Nasiri, M. Khezerloo, N. Laraqi, Numerical investigation of magnetic field effect on mixed convection heat transfer of nanofluid in a channel with sinusoidal walls, J. Magn. Magn. Mater. 401 (2016).
[33] E.E. Tzirtzilakis, N.G. Kafoussias, A. Raptis, Numerical study of forced and free convective boundary layer flow of a magnetic fluid over a flat plate under the action of a localized magnetic field, Z. Angew. Math. Phys. 61 (2010) 5.
[34] H. Aminfar, M. Mohammadpourfard, Y.N. Kahnamouei, A 3D numerical simulation of mixed convection of a magnetic nanofluid in the presence of non-uniform magnetic field in a vertical tube using two phase mixture model, J. Magn. Magn. Mater 323 (2011) 15.
[35] T. Strek, H. Jopek, Computer simulation of heat transfer through a ferrofluid, Phys. Status Solidi (b) 244 (3) (2007).
[36] A. Zeeshan, A. Majeed, R. Ellahi, Effect of magnetic dipole on viscous ferro-fluid past a stretching surface with thermal radiation, J. Mol. Liq. 215 (2016) 549–554.
[37] H.I. Andersson, O.A. Valnes, Flow of a heated Ferrofluid over a stretching sheet in the presence of a magnetic dipole, Acta Mech. 128 (1998).
[38] C.H. Chen, Laminar mixed convection adjacent to vertical, continuously stretching sheets, Heat Mass Transfer 33 (1998) 471–476.